# Keratoconus Diagnosis by Patient-Specific 3D Modelling and Geometric Parameters Analysis

Laurent Bataille[1,2,4,5], Francisco Cavas-Martínez[1(✉)], Daniel G. Fernández-Pacheco[1], Francisco J.F. Cañavate[1], and Jorge L. Alio[3,4,5]

[1] Department of Graphical Expression, Technical University of Cartagena, Cartagena, Spain
{francisco.cavas,daniel.garcia,francisco.canavate}@upct.es
[2] Research and Development Department, Vissum Corporation Alicante, Alicante, Spain
[3] Division of Ophthalmology, Universidad Miguel Hernández, Alicante, Spain
[4] Keratoconus Unit of Vissum Corporation Alicante, Alicante, Spain
[5] Department of Refractive Surgery, Vissum Corporation Alicante, Alicante, Spain
{lbataille,jlalio}@vissum.com

**Abstract.** The aim of this study is to describe a new technique for diagnosing keratoconus based on Patient-specific 3D modelling. This procedure can diagnose small variations in the morphology of the cornea due to keratoconus disease. The posterior corneal surface was analysed using an optimised computational geometric procedure and raw data provided by a corneal tomographer. A retrospective observational case series study was carried out. A total of 86 eyes from 86 patients were obtained and divided into two groups: one group composed of 43 healthy eyes and the other of 43 eyes diagnosed with keratoconus. The predictive value of each morphogeometric variable was established through a receiver operating characteristic (ROC) analysis. The posterior apex deviation variable showed the best keratoconus diagnosis capability (area: 0.9165, $p < 0.000$, std. error: 0.035, 95% CI: 0.846-0.986), with a cut-off value of 0.097 mm and an associated sensitivity and specificity of 89% and 88%, respectively. Patient-specific geometric models of the cornea can provide accurate quantitative information about the morphogeometric properties of the cornea on several singular points of the posterior surface and describe changes in the corneal anatomy due to keratoconus disease. This accurate characterisation of the cornea enables new evaluation criteria in the diagnosis of this type of ectasia and demonstrates that a device-independent approach to the diagnosis of keratoconus is feasible.

**Keywords:** Diagnosis · Geometric modelling · Cornea reconstruction · Scheimpflug · CAD introduction

## 1 Introduction

The analysis of the corneal geometry is critical for the assessment of vision quality in several clinical applications [1, 2]. Consequently, the detection of changes in morphogeometrical properties of the cornea can improve the diagnosis of corneal pathologies [3, 4]. The Keratoconus (KC) is an ectatic corneal disorder usually bilateral but asymmetric. This corneal pathology is most of the time characterised by a corneal thinning


D.-S. Huang et al. (Eds.): ICIC 2017, Part II, LNCS 10362, pp. 176–187, 2017.
DOI: 10.1007/978-3-319-63312-1_16

which results in corneal protrusion, irregular astigmatism and decreased vision [5, 6]. The frequency of occurrence in the general population is low, between 4/1000 and 6/10001. Its prevalence is higher in areas with important exposure to UV light or by a combination of genetic and environmental factors [7].

A significant corneal steepening is observed in the anterior and posterior corneal surfaces and both curvatures are affected in KC eyes and KC suspect eyes [8, 9]. Recent introduction of Scheimpflug photography for corneal topographic characterisation helps in the study and characterisation of both anterior and posterior corneal surfaces [10].

For the diagnosis of ectasia, numerous quantitative descriptors of the corneal surface provided by corneal tomographers can be found in the scientific literature [1, 12]. Recently, a worldwide group of keratoconus experts established the importance of some singular points located at the posterior surface of the cornea for the diagnosis of ectasia [11]. The point of minimum thickness and the highest point (apex or point of maximum curvature) were both defined as the most significative. Nevertheless, none of the quantitative descriptors described above for the diagnosis of ectasias consider these singular points of the posterior corneal surface, so its quantitative description remains a challenge. These descriptors are based on measures such as central corneal thickness, anterior chamber depth, mean simulated keratometry or mean keratometry, among others. Moreover, the values obtained for these descriptors are different depending on the tomographer used [13–16]. This variability prevents their widespread acceptance and clinical utility.

On the other hand several studies, based on Computer-Aided Design (CAD) and Finite Elements (FE), have developed the concept of patient-specific model [17–30]. These patient-specific models are obtained from the so called "raw data" [31], which are generated by systems based on the projection of a slit of light onto the cornea and on the principle of the Scheimpflug photography [1]. These models provide quantitative results relative to the specific cornea of each patient.

The present study demonstrates a new approach for the diagnosis and detection of keratoconus based on the concept of patient-specific 3D modelling and analysis of singular points of each cornea. A validation study was conducted analysing the statistically significant difference of all these singular points between a group of healthy corneas and a group of corneas diagnosed with keratoconus according to Amsler-Krumeich grading system (AK) [32].

## 2 Methods

The Sirius system (CSO, Florence, Italy) was used during the study. It is a non-contact digital rotational Scheimpflug tomographer that represents the entire corneal surface as two discrete and finite sets of spatial point representative of both anterior and posterior corneal surfaces, respectively (Fig. 1a). Point cloud coordinates were exported in a CSV table in polar format. Each row represents a circle on the map with a total of 256 points for each circle (radii are incremented in intervals of 0.2 mm), and each column represents a semi-meridian [33, 34]. In this study, an algorithm was implemented with Matlab

version R2016a (MathWorks, http://www.mathworks.com) to convert the data of the CSV table from polar format to Cartesian format.

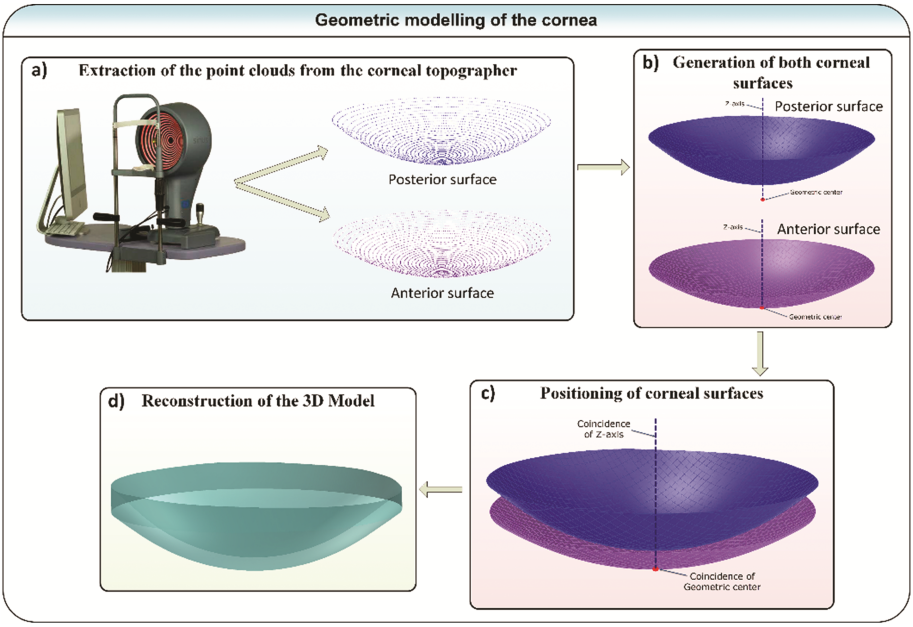


**Fig. 1.** Geometric modelling process by using DGAO tools.

Subsequently, data were imported into the surface reconstruction CAD Rhinoceros [35] version 5.0 software ((MCNeel & Associates, Seattle, USA). Non-uniform rational B-splines (NURBS) were used to generate surfaces, which are characterised by two parametric directions, u and v, that define the spanning process [36, 37]. In this study, the Rhinoceros' surface from the point grid function was applied to the imported point cloud. This function created a rectangular grid of 21 rows and 256 columns, which was deformed in order to minimise the nominal distance between the spatial points and the grid surface (Fig. 1b). The use of this surface reconstruction function permitted obtaining an average deviation error for the posterior surface of the studied corneas with keratoconus (the most irregular corneal surfaces) of about $4.82 \cdot 10^{-16} \pm 5.09 \cdot 10^{-16}$ mm. By using this procedure, the anterior and posterior corneal surfaces were generated and engaged by their geometrical centre and Z axis (Fig. 1c). These surfaces were then joined with the peripheral one (the bonding surface between both sides in the Z-axis direction) to form a single surface.

The surface reconstructed with Rhinoceros was then exported to the SolidWorks v2016 solid modelling software (Dassault Systèmes, Vélizy-Villacoublay, France), which generates the tri-dimensional reconstruction of a solid representative model of the custom and actual geometry of each cornea (Fig. 1d).

Singular points of the posterior surface were then identified on each solid corneal model (healthy or keratoconic), and a morphogeometrical analysis of discrete landmarks

was performed in the local region [38, 39] where curving (caused by progression of keratoconus) manifests gradually.

For this study we analysed the following variables from the posterior surface of the cornea [33, 34]: the Sagittal plane apex area, defined as the area of the cornea within the sagittal plane passing through the Z axis and the highest point (apex, maximum curvature) of the posterior corneal surface (Fig. 2a); Posterior apex deviation (Fig. 2b), defined as the average distance from the Z axis to the highest point (apex, maximum curvature) of the posterior corneal surface; Sagittal plane area at minimum thickness point (Fig. 2c), defined as the area of the cornea within the sagittal plane passing through the Z axis and the minimum thickness point of the posterior corneal surface; Posterior minimum thickness point deviation (Fig. 2d), described as the average distance in the XY plane from the Z axis to the minimum thickness point of the posterior corneal surface. For each cornea, all these variables were measured by the same and unique observer using the SolidWorks calliper function.

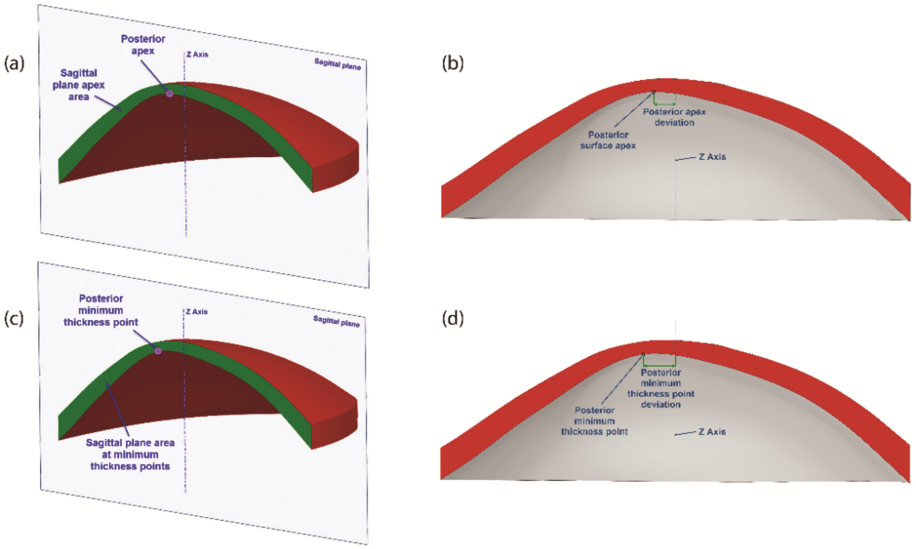


**Fig. 2.** Geometric variables analysed during the study that achieved the best results: (a) sagittal plane apex area, (b) posterior apex deviation, (c) sagittal plane area at minimum thickness point, (d) posterior minimum thickness point deviation.

## 2.1 Statistical Analysis

Data distribution was confirmed by means of the Kolmogorov–Smirnov test. According to this analysis, a Student's t-test was performed in order to test the hypothesis according to the aim of the study. A ROC curve analysis was performed in order to obtain the accuracy of the measurements. A ROC curve is a graphical plot that illustrates the performance of a binary classifier system as its discrimination threshold is varied. The curve is created by plotting the true positive rate against the false positive rate at various

threshold settings. The accuracy of the test depends on how well the test separates the group being tested into those with and without the disease in question. The area under the ROC curve measures the accuracy. A rough guide for classifying the accuracy of a diagnostic test is the traditional academic point system: excellent if 0.90–1; good if 0.80–0.90, fair if 0.70–0.80, and poor if 0.60–0.70. Statistical analyses were performed using Graphpad Prism version 6 software (GraphPad Software, La Jolla, USA) and SPSS version 17.0 software (SPSS, Chicago, USA).

## 3 Results

From a total of 86 patients involved in this study, 43 patients with healthy corneas and aged 12–61 years (36.49 ± 14.86) and 43 patients with keratoconic corneas and aged 17–63 years (38.02 ± 14.98) were modelled. In order to obtain an accurate methodology only initial stages of the disease (stage I), according to Amsler-Krumeich grading, were used during this study. The retrospective study adhered to the tenets of the Declaration of Helsinki and was approved by the local Clinical Research Ethics Committee of Vissum Corporation (Alicante, Spain). Patients examined at Vissum Corporation (Alicante, Spain) were retrospectively enrolled. They were selected from a database of candidates for refractive surgery with normal corneas and also a database of cases diagnosed as having keratoconus in both eyes.

All eyes selected (86) underwent a thorough and comprehensive eye and vision examination which included uncorrected distance visual acuity (UDVA), corrected distance visual acuity (CDVA), manifest refraction, Goldmann tonometry, biometry (IOLMaster, Carl Zeiss Meditec AG) and corneal topographic analysis with the Sirius system® (CSO, Florence, Italy), which is a non-invasive system for measuring and characterizing the anterior segment using a rotating Scheimpflug camera. All measurements were performed by the same experienced optometrists, performing three consecutive measurements and taking average values for the posterior analysis.

**Table 1.** Comparisons within groups (t-tests). Statistical significance (in p-values) between values of different parameters.

| Parameter | Healthy group (M ± SD) | Keratoconus group (M ± SD) | t | p |
|---|---|---|---|---|
| Sagittal plane apex area ($mm^2$) | 4.33 ± 0.27 | 3.90 ± 0.33 | 7.398 | 0.000 |
| Sagittal plane area at minimum thickness point ($mm^2$) | 4.32 ± 0.27 | 3.88 ± 0.33 | 7.563 | 0.000 |
| Posterior apex deviation (mm) | 0.08 ± 0.02 | 0.19 ± 0.09 | -11.271 | 0.000 |
| Posterior minimum thickness point deviation (mm) | 0.80 ± 0.24 | 1.01 ± 0.36 | -3.746 | 0.001 |

M = mean, SD = standard deviation, $N_{Healthy\ group} = 43$, $N_{Keratoconus\ group} = 43$

**Table 2.** Correlations between parameters.

| Parameter | Sagittal plane apex area | Sagittal plane area at minimum thickness point | Posterior apex deviation | Posterior minimum thickness point deviation |
|---|---|---|---|---|
| Sagittal plane apex area | r = 1 | r = 0.998, p < 000 | r = −0.374, p < 000 | r = −0.285, p < 002 |
| Sagittal plane area at minimum thickness point | r = 0.998, p < 000 | r = 1 | r = −0.379, p < 000 | r = −0.295, p < 001 |
| Posterior apex deviation | r = −0.374, p < 000 | r = −0.379, p < 000 | r = 1 | r = 0.475, p < 000 |
| Posterior minimum thickness point deviation | r = −0.285, p < 002 | r = −0.295, p < 001 | r = 0.475, p < 000 | r = 1 |

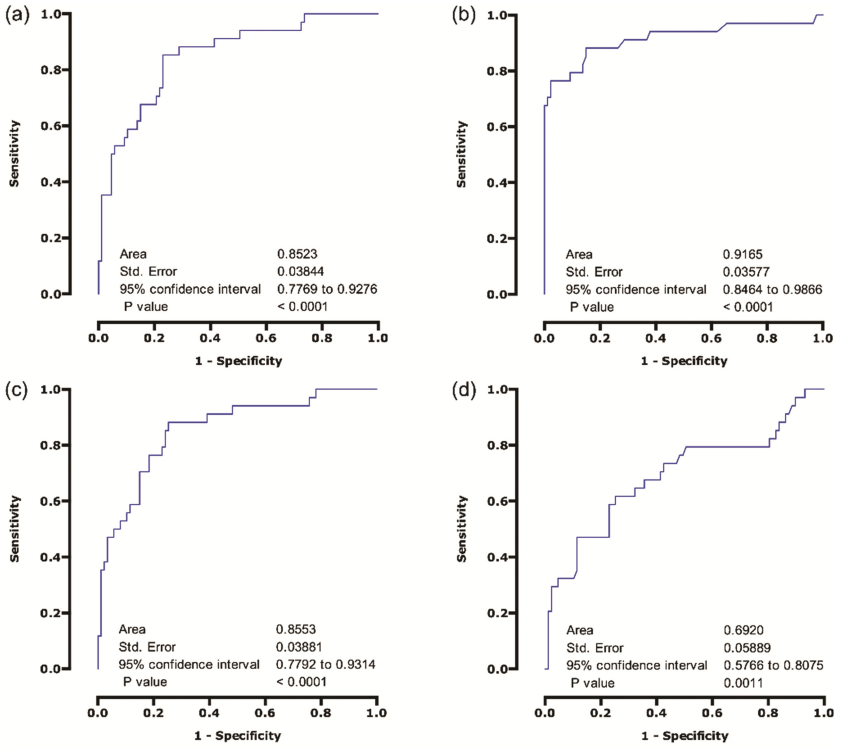


**Fig. 3.** ROC curve modelling sensitivity versus 1-specificity for the variables that diagnosed the existence of keratoconus disease: (a) sagittal plane apex area, (b) posterior apex deviation, (c) sagittal plane area at minimum thickness point, (d) posterior minimum thickness point deviation.

Regarding area parameters, both sagittal plane areas (posterior apex and posterior minimum thickness point) were statistically higher in the subjects with healthy corneas. As expected, minor deviations for the posterior apex and for the posterior minimum thickness point were also observed in the group of normal corneas (see Table 1). A high correlation ($r = 0.998$; $p < 0.000$) between the Sagittal plane apex area and Sagittal plane area at minimum thickness point was also detected (see Table 2).

The predictive value of each morphogeometric parameter was established by a ROC analysis. Four of these parameters offered an area under the curve (AUC) above 0.69 (Fig. 3). The AUC, independent for each variable, appears to demonstrate an adequate sensitivity and specificity classification between groups. The most accurate variable was the posterior apex deviation (Fig. 3b), followed by the sagittal plane area at minimum thickness point (Fig. 3c), sagittal plane apex area (Fig. 3a) and posterior minimum thickness point deviation (Fig. 3d).

## 4 Discussion

This study offers an accurate and realistic method of reconstruction for a biological structure: the human cornea. It creates a new understanding of corneal diseases based on data from the posterior surface, using a robust and cost-effective method based on the generation of a patient-specific 3D model. This computational study provides insight into the complex clinical problem of corneal ectatic disease diagnosis.

In scientific literature, some studies report Computer-Aided Design (CAD) and Finite Elements (FE) models based on the concept of patient-specific analysis. In the Finite Elements field, some reports use these data for several purposes: to predict the response to refractive surgeries [23, 26, 28, 30], the response to intrastromal ring segment implantation in corneas with keratoconus [22], to analyse non-surgical corneal modifications, such as applanation tonometry for intraocular pressure measurement [18, 19, 27, 29] or to analyse the behaviour of corneal tissue properties in different scenarios [17, 20, 21, 24, 25]. In all these cases, raw data were provided by the Pentacam [17–26, 30] (Oculus Optikgeräte GmbH, Wetzlar, Germany), the Sirius [27–29] (CSO, Florence, Italy) or the Galilei [20] (Ziemer Ophthalmic Systems AG, Port, Switzerland) devices. However, due to extrinsic errors [1] that occurred during the measurement process, the generated raw data were incomplete. Therefore, the authors of the mentioned studies decided to interpolate data to obtain a complete image of the corneal surfaces, and thus generating an approximated 3D model of the cornea for its posterior use in the Finite Elements analysis.

In the present study, the raw data obtained also presented the previously mentioned extrinsic errors. However, the authors adopted a design protocol based on geometrical and clinical principles in which only real data were used and not any interpolation was performed [33, 34]. Thus, the patient-specific geometric model generated was an authentic and completely personalised cornea model.

In case of keratoconus the deterioration process of the corneal structure is characterised by a significant reduction of the corneal thickness in comparison to healthy eyes. This is triggered by an alteration in corneal collagen fibres causing stromal thinning and

breaks in the Bowman's membrane during the different stages of the disease [5, 40]. Furthermore, the presence of corneal irregularities and the influence of the intraocular pressure on these weakened structures will create local steepening and increased radius of curvature which will lead to an increased posterior corneal surface area [5, 6, 40, 41]. In the keratoconus group, the sagittal plane areas were smaller because of their local structural weakening due to fewer collagen fibres in each lamella and the influence of the intraocular pressure [6]. These values are consistent with those published by different studies [41, 42] which have reported that in irregular corneal areas the geometry of posterior corneal surfaces were affected due to the lower number of stromal lamellae and the smaller lamellar interconnection. In other studies where a similar characterisation of the corneas has been described for the differentiation of pathologic eyes, the variables related to corneal thickness and volume, among others, are directly given by the software of the topographers [43–46]. However, in the present study the morpho-geometric variables are calculated from a 3D model generated using only real and non-interpolated raw point cloud data provided by the tomographer.

The average distance from the Z axis to the apex of the posterior corneal surface (deviation of the apex point of posterior corneal surface) differed between groups, with the largest deviations found in the group of eyes with keratoconus. The deviation of the apex on the posterior surface of the cornea was larger in the eyes with keratoconus ($0.19 \pm 0.09$ mm), and there was also a slight deviation in healthy corneas ($0.08 \pm 0.02$ mm) according to the toricity manifested in the subjective refraction [47]. The aforementioned presence of an irregular corneal surface, which created a protrusion in the keratoconic eye, also led to an increased corneal curvature [48] and, therefore, to an increase in the deviation of the point of minimum thickness (maximum curvature) of the posterior corneal surface (average distance from the Z axis to the minimum thickness point of the posterior corneal surface). These deviations were greater in the eyes with keratoconus ($1.01 \pm 0.36$ mm) compared with healthy eyes ($0.80 \pm 0.24$ mm). Some researchers have evaluated certain corneal irregularity ratios and concluded that they were higher for keratoconic corneas [49–51].

The analysis of these variables concluded that the parameter that provides a higher discrimination rate between normal corneas and corneas with keratoconus was the posterior apex deviation (ROC area: 0.9165, $p < 0.000$, std. error: 0.035, 95% CI: 0.846–0.986), with a cut-off value of 0.097 mm and an associated sensitivity and specificity of 89% and 88%, respectively. This is justified due to the structural instability that keratoconic corneas present in its architecture, being the posterior surface the most susceptible to variations given the forces exerted on the tissue. Several studies have concluded the importance of, and interest in, the posterior corneal surface [50]. However, to the authors' knowledge, this is the first study to describe this phenomenon in disease stage when the degree of corneal protrusion is apparent in the posterior corneal surface, which supports the diagnosis accuracy of the proposed method.

Furthermore, the non-invasive clinical diagnosis method proposed in this study develops the concept of interoperability [52]: a new methodology that uses raw data, which can be shared among the corneal topographers that are based on the projection of a slit of light onto the cornea and on the principle of Scheimpflug photography.

This exchange of information could imply a common benefit for the whole ophthalmic community.

## 5 Conclusion

In summary, this method provides a feasible and new diagnostic approach of keratoconus, using raw elevation data from any corneal tomographer without the need of proprietary internal algorithms and quantifying the singular points of the posterior corneal surface for diagnosing keratoconus. It is in agreement with the main conclusions drawn by the group of world experts in keratoconus. It also offers a potential comparative tool to analyze data from corneal tomographers from different manufacturers allowing data sharing. This could lead to a better understanding of the ethology and prognosis of this eye disease.

In future studies, our objective will be to increase the number of eyes in each group, to carry out a more advanced statistical analysis and to compare the results with the commercially available multiparametric keratoconus detection indexes.

In future applications, the same method could be used to improve the detection and effects of therapeutic methods used for different grades of keratoconus and other corneal ectatic diseases, such as post-LASIK ectasia.

## References

1. Cavas-Martinez, F., De la Cruz Sanchez, E., Nieto Martinez, J., Fernandez Canavate, F.J., Fernandez-Pacheco, D.G.: Corneal topography in keratoconus: state of the art. Eye **3**, 5 (2016). (Lond)
2. Arnalich-Montiel, F., Alio Del Barrio, J.L., Alio, J.L.: Corneal surgery in keratoconus: which type, which technique, which outcomes? Eye Vis. **3**, 2 (2016). (London, England)
3. Montalban, R., Alio, J.L., Javaloy, J., Pinero, D.P.: Correlation of anterior and posterior corneal shape in keratoconus. Cornea **32**, 916–921 (2013)
4. Belin, M.W., Ambrosio, R.: Scheimpflug imaging for keratoconus and ectatic disease. Indian J. Ophthalmol. **61**, 401–406 (2013)
5. Rabinowitz, Y.S.: Keratoconus. Surv. Ophthalmol. **42**, 297–319 (1998)
6. Pinero, D.P., Alio, J.L., Barraquer, R.I., Michael, R., Jimenez, R.: Corneal biomechanics, refraction, and corneal aberrometry in keratoconus: an integrated study. Invest. Ophthalmol. Vis. Sci. **51**, 1948–1955 (2010)
7. Rabinowitz, Y.S., Barbara, A.: Epidemiology of keratoconus. In: Textbook on Keratoconus New Insights (2012)
8. Wilson, S.E., Lin, D.T., Klyce, S.D.: Corneal topography of keratoconus. Cornea **10**, 2–8 (1991)
9. Tomidokoro, A., Oshika, T., Amano, S., Higaki, S., Maeda, N., Miyata, K.: Changes in anterior and posterior corneal curvatures in keratoconus. Ophthalmology **107**, 1328–1332 (2000)
10. Dubbelman, M., Sicam, V.A., Van der Heijde, G.L.: The shape of the anterior and posterior surface of the aging human cornea. Vis. Res. **46**, 993–1001 (2006)

11. Gomes, J.A., Tan, D., Rapuano, C.J., Belin, M.W., Ambrosio Jr., R., Guell, J.L., Malecaze, F., Nishida, K., Sangwan, V.S.: Global consensus on keratoconus and ectatic diseases. Cornea **34**, 359–369 (2015)
12. Belin, M.W., Duncan, J.K.: Keratoconus: the ABCD grading system. Klin. Monatsbl. Augenheilkd. **233**, 701–707 (2016)
13. Anayol, M.A., Guler, E., Yagci, R., Sekeroglu, M.A., Ylmazoglu, M., Trhs, H., Kulak, A.E., Ylmazbas, P.: Comparison of central corneal thickness, thinnest corneal thickness, anterior chamber depth, and simulated keratometry using galilei, Pentacam, and Sirius devices. Cornea **33**, 582–586 (2014)
14. Hernandez-Camarena, J.C., Chirinos-Saldana, P., Navas, A., Ramirez-Miranda, A., de la Mota, A., Jimenez-Corona, A., Graue-Hernindez, E.O.: Repeatability, reproducibility, and agreement between three different Scheimpflug systems in measuring corneal and anterior segment biometry. J. Refract. Surg. **30**, 616–621 (2014). (Thorofare, N.J.1995
15. Savini, G., Carbonelli, M., Sbreglia, A., Barboni, P., Deluigi, G., Hoffer, K.J.: Comparison of anterior segment measurements by 3 Scheimpflug tomographers and 1 Placido corneal topographer. J. Cataract Refract. Surg. **37**, 1679–1685 (2011)
16. Shetty, R., Arora, V., Jayadev, C., Nuijts, R.M., Kumar, M., Puttaiah, N.K., Kummelil, M.K.: Repeatability and agreement of three Scheimpflug-based imaging systems for measuring anterior segment parameters in keratoconus. Invest. Ophthalmol. Vis. Sci. **55**, 5263–5268 (2014)
17. Ariza-Gracia, M.Á., Redondo, S., Llorens, D.P., Calvo, B., Rodriguez Matas, J.F.: A predictive tool for determining patient-specific mechanical properties of human corneal tissue. Comput. Methods Appl. Mech. Eng. **317**, 226–247 (2017)
18. Ariza-Gracia, M.A., Zurita, J., Pinero, D.P., Calvo, B., Rodriguez-Matas, J.F.: Automatized patient-specific methodology for numerical determination of biomechanical corneal response. Ann. Biomed. Eng. **44**, 1753–1772 (2016)
19. Ariza-Gracia, M.A., Zurita, J.F., Pinero, D.P., Rodriguez-Matas, J.F., Calvo, B.: Coupled biomechanical response of the cornea assessed by non-contact tonometry. A simulation study. PLoS ONE **10**, e0121486 (2015)
20. Asher, R., Gefen, A., Moisseiev, E., Varssano, D.: An analytical approach to corneal mechanics for determining practical, clinically-meaningful patient-specific tissue mechanical properties in the rehabilitation of vision. Ann. Biomed. Eng. **43**, 274–286 (2015)
21. Dupps Jr., W.J., Seven, I.: A large-scale computational analysis of corneal structural response and ectasia risk in myopic laser refractive surgery. Trans. Am. Ophthalmol. Soc. **114**, T1 (2016)
22. Lago, M.A., Ruperez, M.J., Monserrat, C., Martinez-Martinez, F., Martinez-Sanchis, S., Larra, E., Diez-Ajenjo, M.A., Peris-Martinez, C.: Patient-specific simulation of the intrastromal ring segment implantation in corneas with keratoconus. J. Mech. Behav. Biomed. Mater. **51**, 260–268 (2015)
23. Lanchares, E., Del Buey, M.A., Cristobal, J.A., Calvo, B.: Computational simulation of scleral buckling surgery for rhegmatogenous retinal detachment: on the effect of the band size on the myopization. J. Ophthalmol. **2016**, 3578617 (2016)
24. Roy, A.S., Dupps Jr., W.J.: Patient-specific computational modeling of keratoconus progression and differential responses to collagen cross-linking. Invest. Ophthalmol. Vis. Sci. **52**, 9174–9187 (2011)
25. Seven, I., Roy, A.S., Dupps Jr., W.J.: Patterned corneal collagen crosslinking for astigmatism: computational modeling study. J. Cataract Refract. Surg. **40**, 943–953 (2014)

26. Seven, I., Vahdati, A., De Stefano, V.S., Krueger, R.R., Dupps Jr., W.J.: Comparison of patient-specific computational modeling predictions and clinical outcomes of LASIK for Myopia. Invest. Ophthalmol. Vis. Sci. **57**, 6287–6297 (2016)
27. Simonini, I., Angelillo, M., Pandolfi, A.: Theoretical and numerical analysis of the corneal air puff test. J. Mech. Phys. Solids **93**, 118–134 (2016)
28. Simonini, I., Pandolfi, A.: Customized finite element modelling of the human cornea. PLoS ONE **10**, e0130426 (2015)
29. Simonini, I., Pandolfi, A.: The influence of intraocular pressure and air jet pressure on corneal contactless tonometry tests. J. Mech. Behav. Biomed. Mater. **58**, 75–89 (2016)
30. Vahdati, A., Seven, I., Mysore, N., Randleman, J.B., Dupps Jr., W.J.: Computational biomechanical analysis of asymmetric ectasia risk in unilateral Post-LASIK ectasia. J. Refract. Surg. **32**, 811–820 (2016). (Thorofare, N.J.1995)
31. Ramos-Lopez, D., Martinez-Finkelshtein, A., Castro-Luna, G.M., Pinero, D., Alio, J.L.: Placido-based indices of corneal irregularity. Optom. Vis. Sci. **88**, 1220–1231 (2011)
32. Amsler, M.: Keratocone classique et keratocone fruste, arguments unitaries. Ophthalmologica **111**, 96–101 (1946). Journal international d'ophtalmologie. International journal of ophthalmology. Zeitschrift für Augenheilkunde
33. Cavas-Martinez, F., Fernandez-Pacheco, D.G., De la Cruz-Sanchez, E., Martinez, N.J., Fernandez Canavate, F.J., Vega-Estrada, A., Plaza-Puche, A.B., Alio, J.L.: Geometrical custom modeling of human cornea in vivo and its use for the diagnosis of corneal ectasia. PLoS ONE **9**, e110249 (2014)
34. Cavas-Martínez, F., Fernández-Pacheco, D.G., De La Cruz-Sánchez, E., Martínez, J.N., Cañavate, F.J.F., Alio, J.L.: Virtual biomodelling of a biological structure: the human cornea. Dyna **90**, 647–651 (2015)
35. Browning, J.E., McMann, A.K.: Computational engineering: design, development and applications (2012)
36. Espinosa, J., Mas, D., Pérez, J., Illueca, C.: Optical surface reconstruction technique through combination of zonal and modal fitting. J. Biomed. Opt. **15**, 026022 (2010)
37. Piegl, L.A., Tiller, W.: Approximating surfaces of revolution by nonrational B-splines. IEEE Comput Graph. Appl. **23**, 46–52 (2003)
38. Benítez, H.A., Püschel, T.A.: Modelling shape variance: geometric morphometric applications in evolutionary biology. Int. J. Morphol. **32**, 998–1008 (2014)
39. Klingenberg, C.P.: Analyzing fluctuating asymmetry with geometric morphometrics: concepts, methods, and applications. Symmetry **7**, 843–934 (2015)
40. Parker, J.S., van Dijk, K., Melles, G.R.J.: Treatment options for advanced keratoconus: a review. Surv. Ophthalmol. **60**, 459–480 (2015)
41. Sherwin, T., Brookes, N.H., Loh, I.P., Poole, C.A., Clover, G.M.: Cellular incursion into Bowman's membrane in the peripheral cone of the keratoconic cornea. Exp. Eye Res. **74**, 473–482 (2002)
42. Ozgurhan, E.B., Kara, N., Yildirim, A., Bozkurt, E., Uslu, H., Demirok, A.: Evaluation of corneal microstructure in keratoconus: a confocal microscopy study. Am. J. Ophthalmol. **156**, 885–893 (2013). e882
43. Emre, S., Doganay, S., Yologlu, S.: Evaluation of anterior segment parameters in keratoconic eyes measured with the Pentacam system. J. Cataract Refract. Surg. **33**, 1708–1712 (2007)
44. Ambrosio Jr., R., Alonso, R.S., Luz, A., Velarde, L.G.C.: Corneal-thickness spatial profile and corneal-volume distribution: tomographic indices to detect keratoconus. J. Cataract Refract. Surg. **32**, 1851–1859 (2006)

45. Cervino, A., Gonzalez-Meijome, J.M., Ferrer-Blasco, T., Garcia-Resua, C., Montes-Mico, R., Parafita, M.: Determination of corneal volume from anterior topography and topographic pachymetry: application to healthy and keratoconic eyes. Ophthalmic Physiol. Optics **29**, 652–660 (2009). the journal of the British College of Ophthalmic Opticians (Optometrists)
46. Mannion, L.S., Tromans, C., O'Donnell, C.: Reduction in corneal volume with severity of keratoconus. Curr. Eye Res. **36**, 522–527 (2011)
47. Montalban, R., Pinero, D.P., Javaloy, J., Alio, J.L.: Correlation of the corneal toricity between anterior and posterior corneal surfaces in the normal human eye. Cornea **32**, 791–798 (2013)
48. Ozcura, F., Yildirim, N., Tambova, E., Sahin, A.: Evaluation of Goldmann applanation tonometry, rebound tonometry and dynamic contour tonometry in keratoconus. J. Optom. **10**, 117–122 (2016)
49. Safarzadeh, M., Nasiri, N.: Anterior segment characteristics in normal and keratoconus eyes evaluated with a combined Scheimpflug/Placido corneal imaging device. J. Curr. Ophthalmol. **28**, 106–111 (2016)
50. Schlegel, Z., Hoang-Xuan, T., Gatinel, D.: Comparison of and correlation between anterior and posterior corneal elevation maps in normal eyes and keratoconus-suspect eyes. J. Cataract Refract. Surg. **34**, 789–795 (2008)
51. Tanabe, T., Tomidokoro, A., Samejima, T., Miyata, K., Sato, M., Kaji, Y., Oshika, T.: Corneal regular and irregular astigmatism assessed by Fourier analysis of videokeratography data in normal and pathologic eyes. Ophthalmology **111**, 752–757 (2004)
52. ISO/IEC/IEEE International Standard - Systems and software engineering – Life cycle processes –Requirements engineering. ISO/IEC/IEEE 29148:2011(E), pp. 1–94 (2011)